World Academy of Science, Engineering and Technology
International Journal of Materials and Metallurgical Engineering
Vol:17, No:3, 2023

Mechanical Properties of D2 Tool Steel Cryogenically Treated Using Controllable Cooling

A. Rabin, G. Mazor, I. Ladizhenski, R. Z. Shneck

***Abstract*—**The hardness and hardenability of AISI D2 cold work tool steel with conventional quenching (CQ), deep cryogenic quenching (DCQ) and rapid deep cryogenic quenching heat treatments caused by temporary porous coating based on magnesium sulfate was investigated. Each of the cooling processes was examined from the perspective of the full process efficiency, heat flux in the austenite-martensite transformation range followed by characterization of the temporary porous layer made of magnesium sulfate using confocal laser scanning microscopy (CLSM), surface and core hardness and hardenability using Vickers hardness technique. The results show that the cooling rate (CR) at the austenite-martensite transformation range has a high influence on the hardness of the studied steel.

***Keywords*—**AISI D2, controllable cooling, magnesium sulfate coating, rapid cryogenic heat treatment, temporary porous layer.

I. Introduction

THE AISI D2 steel is a high chromium (Cr), high carbon (C), tool and die steel used for cold working operations and can be hardened to 721.5 ± 24.5 HV (61 ± 1 HRC) before tempering and to 646 ± 51 HV (57.5 ± 2.5 HRC) after double tempering cycle (conversion of hardness values from HRC to HV and vice versa were performed according to ASTM E140-12b, Table I). The recommended heat treatment of AISI D2 tool steel can be seen in Fig. 1 [1]. This steel is one of most extensively studied martensitic steel subjected to Deep Cryogenic Treatment (DCT) [2]-[11], in which cryogenic treatment produces higher mechanical properties compared to quenching to room temperature.

Increasing the carbon concentration lowers the martensite start (M_s) and martensite finish (M_f) temperatures and increases the amounts of retained austenite [12]. To eliminate the retained austenite after water, air and brine quenching, a cryogenic treatment is needed.

The austenite to martensite transformation is a diffusionless, athermal process [12]. Although the lowest temperature is the main parameter that determines the amount of transformation, the CR at the austenite-martensite transformation range has a very important role. If the CR is slow enough, the austenite will have enough time to stabilize and some of the austenite will remain within the martensitic phase [12]. Therefore, the residual austenite can be eliminated by very high CR or by leaving the workpiece inside the cryogenic media for a long time, making the hardening process inefficient in terms of time and resource consumption.

The importance of high CR was manifested in 1964 by Kobasko who suggested the Intensive Quenching (IQ) process, in which the CR during quenching is enhanced compared to a traditional heat treatment of steels [49]. This process may provide better workpiece characteristic, such as fatigue resistance, impact strength, hardenability, reduction of crack formation probability, minimizing the distortion and the residual stress of a metallic workpiece.

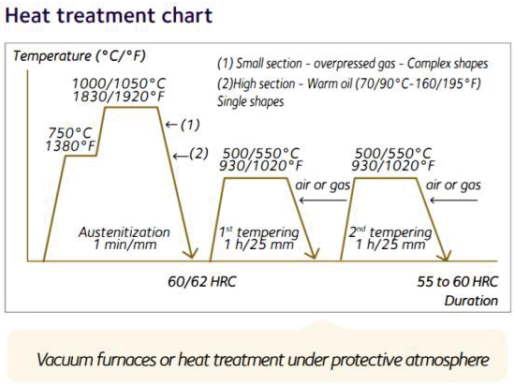

Fig. 1 Common heat treatment for hardening an AISI D2 tool steel

The principle of IQ technique is explained by the interplay between the surface of the part being quenched and the core. The core is in an expanded state since its temperature is always higher than the surface. Upon transforming to martensite its volume increases by additional 4 vol%. On the other hand, the surface is cooler and therefore it starts in a contracted state, until its temperature decreases below M_s, then it transforms and expands by 4 vol%. At the beginning of quenching the contraction gives rise to tensile stresses at the surface, which may cause danger of cracking. Once its temperatures reduce below M_s the stresses turn to compression and the danger of cracking is prevented. The essence of the intensive cooling is to cool the surface fast enough below M_s in order to generate compressive stresses before cracking takes place. That is, the higher CR, the greater the chance to prevent quench cracking [13], [14].

Process continuity is another feature that affects the amount

Andrey Rabin is with the Materials Engineering Department, Ben-Gurion University of the Negev, David Ben Gurion Blvd 1, Beer-Sheva, 84105 Israel and with the Nuclear Research Center Negev (NRCN), Beer-Sheva 84190, Israel (corresponding author, phone: +927506238935; e-mail: andreyra@post.bgu.ac.il).

Gedalya Mazor and Izhak Ladizhensky are with the Mechanical Engineering Department, Shamoon College of Engineering, Haim Nachman Bialik St 56, Beer-Sheva, 84100, Israel (e-mail: mazorg@sce.ac.il, izhak@sce.ac.il).).

Roni Zvi Shneck is with the Materials Engineering Department, Ben-Gurion University of the Negev, David Ben Gurion Blvd 1, Beer-Sheva, 84105 Israel (e-mail: roni@bgu.ac.il).

of residual austenite. By stopping (holding) the cooling at a higher temperature then the required cryogenic temperature, the austenite stabilizes and upon re-starting the cooling, the transformation of the austenite to martensite will start at lower temperature. Moreover, there is a chance that the transformation from austenite to martensite will never be completed [15].

One of the main reasons which affects low CR in a cryogenic environment is the 'pool boiling' phenomenon, which is the boiling process over hot body in a cold liquid without forced movement. Steam pockets form on the hot surface until they are large enough. At this moment, they disconnect from the hot surface and rise in the form of bubbles. The boiling process takes place in the entire volume of the liquid. There are many factors affecting boiling such as: the nature of the hot body surface, its dimensions, the thermophysical properties of the liquid and the vapor, the pressure and the heat flux (HF) [16]-[18].

In order to achieve the highest HF during the cryogenic heat treatment, 'transition boiling' and 'film boiling' regimes have to be shortened as much as possible or even eliminated completely. The methods of enhancing the HF can be divided into two groups of active and passive methods [19], [20]. Active methods involve external power investment for the enhancement in heat transfer; for examples vibrating the liquid or the heated component within the liquid, circulating the liquid or the component within the liquid, creating electrostatic and ultrasonic fields, pumping steam from the wall of the component, vigorous water spray and other methods [21]-[25]. These active methods require considerable investment of energy and are relatively expensive. Passive methods do not require a constant external power, for example modifying the quenching liquid media, using additives and nanofluids [26] and modifying the surface of the workpiece, by machining or grooving, formed or modified low-fin surfaces, multi layered surfaces or coated surfaces [27].

The main purpose of coated surfaces is to provide structural changes at the surface of the workpiece which are used to increase the surface area and physically to break the film boiling layer. The coatings can be done by different techniques and materials, such as: sintering [28], bonding with inter-material compounds [29], electrochemical deposition [30], dry-etching [31], microelectromechanical systems (MEMS) [32] technique and others.

A thin porous layer coating has been proven to be especially effective as a passive enhancer of critical HF (CHF) [33]. This is thought to be a result of a combination of an extended surface area effect, a capillary-assist to liquid flow effect, an increased nucleation site density effect and the vapor escape paths from the porous layer [33]. During the past years, the porous layer coating technique was researched using different pour structure, uniformity and a lot of different modifications [34]-[37]. Although micro or nano porous layer coatings can provide tremendous improvement in heat transfer, most of them can be produced in research laboratories and only for individual components, preventing their use on an industrial scale. One of the other problems that exist in the use of porous coatings is the fact that most of the layers are permanent and cannot be removed from the surface of the workpiece by simple methods, so they cause a change in the workpiece final dimensions, or its mechanical or chemical properties over the surface.

So far, much research was done on heat transfer enhancement using porous layer coating during traditional quenching, into media, such as, oil, water and brine etc. Not much work [38]-[40], was found in the field of cryogenic environment, especially of using porous layer coatings [41]-[45]. There are several requirements in order for the process to be economically efficient, namely:

- The porous layer coating must provide high HF along the necessary cryogenic heat treatment temperatures range.
- The price of the coating material has to be relatively low.
- The coating formation method has to be relatively easy and economically efficient.
- The coating layer should be such that at the end of the treatment process it can be removed by simple means.

This research is concentrated on the creation of a temporary porous layer coating based on dipping the workpiece inside magnesium sulfate solution, which can be removed by simple means, using tap water that dissolves the coating at the end of the process.

II. Experimental

A. Materials

The temporary coating material was a magnesium sulfate heptahydrate ($MgSO_4$-$7H_2O$) with commercial purity. Chemical analysis and technical specification are listed in Table I.

TABLE I
CHEMICAL ANALYSIS AND TECHNICAL SPECIFICATION OF MAGNESIUM SULFATE

Magnesium Sulfate Heptahydrate 99.5%	
Magnesium Sulfate ($MgSO_4$)	50-51%
Magnesium Oxide (MgO)	16-17%
Sulphur Trioxide (SO_3)	30-32%
Lol	49-50%
CAS	7487-88-9
Humidity (for 25°C)	0.1%
pH	7.0-7.5
Appearance	White Crystallized Solid
Solubility	In water
Molecular Weight	246.48 g/mol

The investigated steel was a commercial AISI D2 cold work tool steel which was cut from a single rod and its composition was analyzed by optical emission spectrometer (ASTM-E-1066-2008) and listed in Table II.

TABLE II
CHEMICAL COMPOSITION OF THE STUDIED AISI D2 TOOL STEEL

Element	Fe	C	Mn	Si	Cr	Mo	P	Cu	S
Content [%]	Balance	1.51	0.6	0.37	11.31	0.76	0.024	0.23	0.003

The continuous cooling transformation (CCT) and time-temperature-transformation (TTT) diagrams were determined using the JMatPro v.7.0.0 Material Property Simulation

Package based on the chemical composition of the material and are shown in Figs. 2 (a) and (b) respectively. The simulated diagrams predict that M_s = 68.2 °C, M_{50} = 21.3 °C and M_{90} = -87.6 °C. The equilibrium phase composition of AISI D2 tool steel is presented in Fig. 2 (c) according to [46].

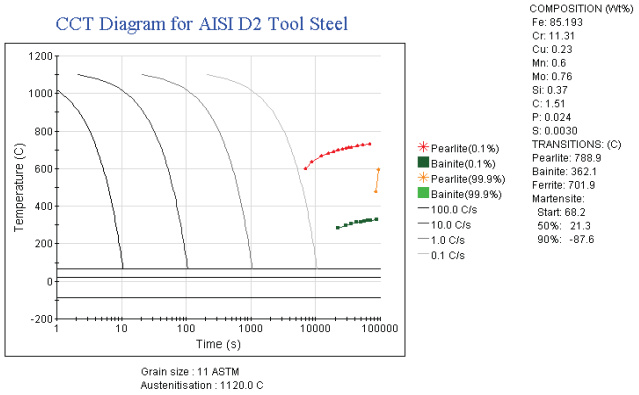

(a)

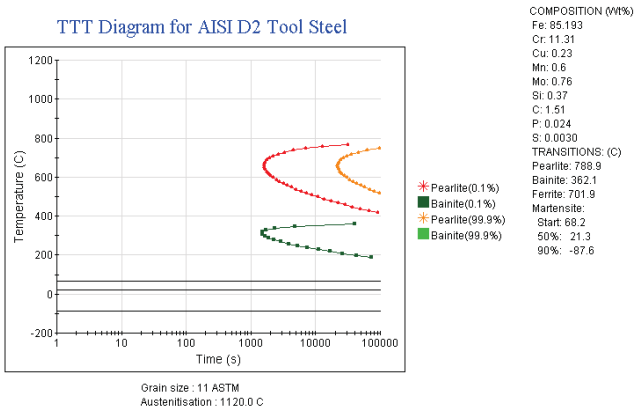

(b)

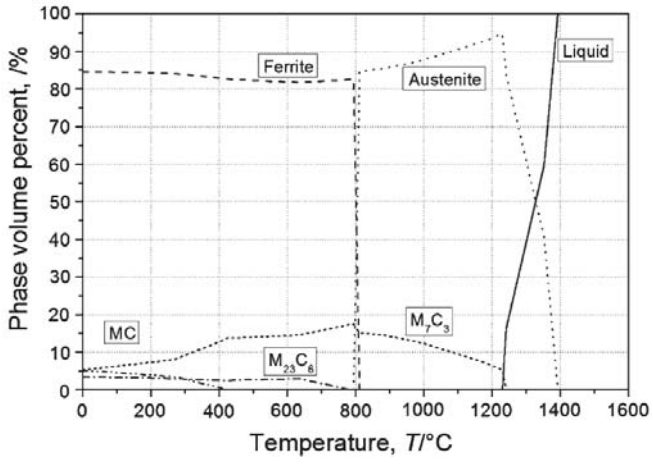

(c)

Fig. 2 (a) CCT and (b) TTT diagrams based on the chemical composition of the material using a JMatPro v.7.0.0 Material Property Simulation Package (c) Equilibrium diagram for AISI D2 tool steel

The specimens were cut into cylinders with a dimension of ∅30x30 mm. Then, a 3.6 mm diameter hole was drilled in the center of the specimen, to a depth of 15 mm and a type K thermocouple was implant in the hole. An illustration of the specimen can be seen in Fig. 3.

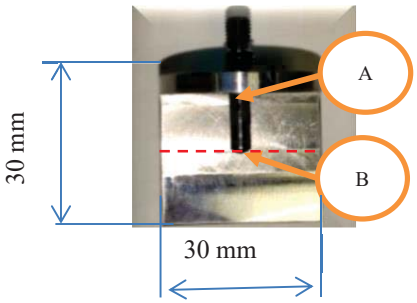

Fig. 3 The thermocouple position (A) inside the specimen (the specimen was vertically cross sectioned to illustrate the contact point B

B. Characterization Methods

The morphology of the porous layer obtained by the magnesium sulfate solution was characterized by CLSM using Olympus OLS500 SAF 3D microscope with MPLFLN10xLEXT objective lens. Two different specimens subjected to different porous layer creation procedures were characterized. In each specimen a single strip along the surface of the layer was chosen randomly and scanned. In addition, on each strip of the layer at the top and bottom, smaller areas were selected for inspection at higher resolution.

Near surface and core hardening measurements were performed using Zwick/Roell ZHV30-s with Vickers pyramid-shaped diamond indenter, and an applied load of 10 kgf (98.1 N) with a 10 sec indentation dwell time. Each specimen was polished up to 400 P grit SiC paper. For near surface hardness test, each specimen underwent a hardness test along a diameter of the basal plane. Five points were marked at distances of ~5 mm and at each point two tests were performed. An example of the test locations is shown in Fig. 4.

Fig. 4 On surface hardness test locations

To estimate the hardenability, each specimen was cut at its mid-height (~15 mm from the bottom point, along the red line in Fig. 3) by EDM using ARTA 123 PRO EDM cutting machine with ∅0.25 mm Brass wire at a rate of 4 mm/min. Each specimen was polished and underwent hardness tests as

described above.

C. Experimental System

The experimental system configuration is shown in Fig. 5.

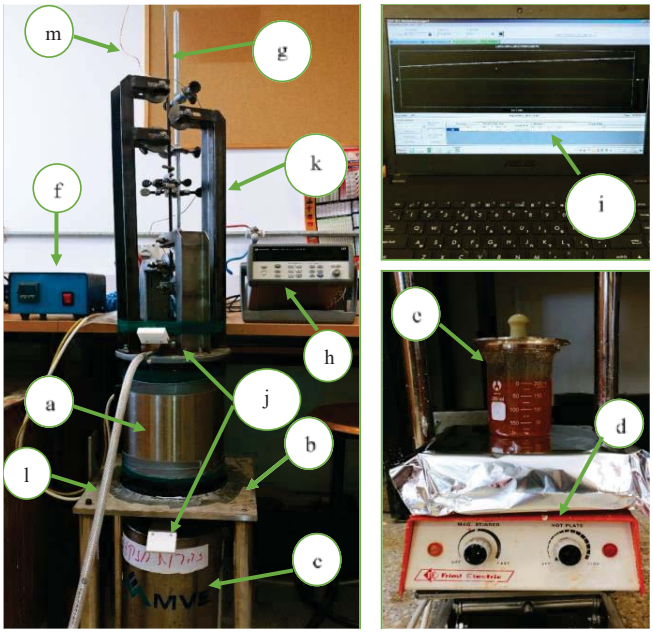

Fig. 5 Experimental system

The set up contains: (a) Tubular air resistance-heating furnace for temperatures up to 1,200 °C with inner diameter of 40 mm, (b) A metallic base to hold the furnace above the Dewar with the liquid nitrogen or the chemical cup with magnesium sulfate solution, (c) Metallic Dewar, containing the liquid nitrogen, (d) Heating tray with stirrer to mix magnesium sulfate solution, (e) A 250/2,500 cc chemical cup containing magnesium sulfate solution to create the porous layer, (f) Temperature controller of the oven, (g) A tube that fixes the specimen and transmits the specimen thermocouple. The tube ensures vertical and straight movement of the specimen, (h) A data logger (KEYSIGHT 34972A) for the continuous thermocouple temperature measurements, (i) Computer with data processing software (Agilent), (j) Metal shutters to seal the oven from heat leakage and air entry, (k) A device that centralizes the movement of the specimen, (l) A pipe that carries the protecting argon gas, and (m) A K type thermocouple implanted in the center of the specimen.

D. Temporary Porous Layer Optimization Procedures

Two series of experiments were performed to find optimal conditions for obtaining temporary porous coating layers based on magnesium sulfate as follows:

- Temporary porous layer creation prior the austenitizing stage, in which the specimen was heated to different initial temperatures (250 °C, 300 °C and 350 °C), dipped for different periods of time (1 sec, 3 sec and 5 sec) in boiling magnesium sulfate solution with different concentrations (20%, 30%, 40% and 50wt.%$MgSO_4$-$7H_2O$). The results of this procedure yield different morphologies and thicknesses of the coatings. After receiving the coating, the specimen was heated up to approximately 830 °C inside a tubular furnace and immediately submerged into a Dewar flask filled with liquid nitrogen until the specimen reaches the Liquid Nitrogen (LN2) boiling temperature (-196 °C). Two examples of cooling curves (T-t) obtained using different morphologies of temporary porous layer coatings can be seen in Fig. 6 and an example of the appearance as function of coating forming conditions can be seen in Table III.

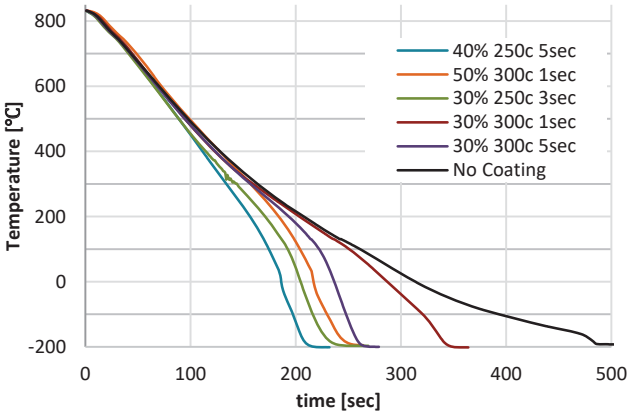

Fig. 6 Examples of cooling curves (T-t) obtained using different morphologies of temporary porous layer created prior to austenitizing stage coatings based on magnesium sulfate solution concentration, initial specimen dipping temperature and the dipping time of the specimen inside the solution

TABLE III
EXAMPLE OF COATING FORMING CONDITIONS AND ITS MORPHOLOGY PRIOR THE AUSTENITIZING STAGE

Coating forming conditions	Solution concentration [%]	40	30	50	30	30
	Initial dipping temperature [°C]	250	250	300	300	300
	Dipping time [s]	5	3	1	1	5
Temporary porous layer morphology						

- Temporary porous layer creation during the quenching stage, in which the specimen was heated up to 1,120 °C, immersed into magnesium sulfate solution (which was at room temperature) with different concentrations (20%,

30% and 40wt.%$MgSO_4$-7H_2O). When the specimen was cooled down to a predetermined temperature (250 °C, 300 °C, 350 °C and 400 °C) it was pulled out from the solution. The results of this procedure yield different morphologies and thicknesses of the coatings. After pulling out from the magnesium sulfate solution, the specimen was immediately submerged into a Dewar flask filled with LN2 until reaching -196 °C. Examples of cooling curves obtained using different morphologies of temporary porous layer coatings produced in the second procedure are presented in Fig. 7 and examples of their appearance as function of coating forming conditions are shown in Table IV.

The conditions for obtaining a porous layer which produced the highest CR were found to be 40wt.%$MgSO_4$-7H_2O in boiling solution, initial dipping temperature of 250 °C and holding for 3 seconds and 40wt.%$MgSO_4$-7H_2O in room temperature solution and removal temperature of the specimen from the solution of 350 °C for the temporary porous layer creation during the quenching stage.

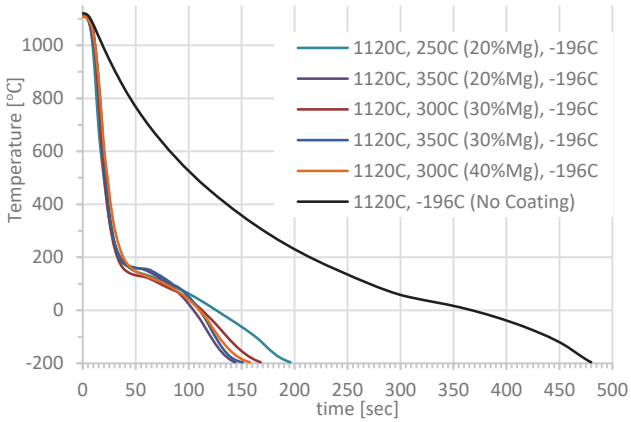

Fig. 7 Examples of cooling curves obtained using different morphologies of temporary porous layer coatings produced in the second procedure, fate solution created during the quenching stage

TABLE IV
EXAMPLE OF COATING FORMING CONDITIONS AND ITS MORPHOLOGY DURING THE QUENCHING STAGE

Coating forming conditions						
	Solution concentration [%]	20	20	30	30	40
	final dipping temperature [°C]	250	350	300	350	300
Temporary porous layer morphology						

TABLE V
DESCRIPTION OF THE HEAT PROCESSES

Heat treatment	Description
AR	As received specimen without any heat treatment.
WQ	Water quenching - Heating up to 1,120 °C for 30 min, quenching in tap water down to ~25 °C.
CQ	Cryogenic quenching - Heating up to 1,120 °C for 30 min, quenching in liquid nitrogen down to ~-196 °C.
WCQ	Water and cryogenic quenching - Heating up to 1,120 °C for 30 min, quenching in tap water down to ~350 °C, quenching in liquid nitrogen down to ~-196 °C.
SCQ1	Magnesium sulfate and cryogenic quenching 1 – Heating up to 1,120 °C for 30 min, quenching in 40wt.%$MgSO_4$-7H_2O (room temperature) solution down to ~350 °C, quenching in liquid nitrogen down to ~-196 °C.
SCQ2	Magnesium sulfate and cryogenic quenching 2 – Heating up to 250 °C, dipping inside 40wt.%$MgSO_4$-7H_2O boiling solution for 3 sec, heating up to 1,120 °C for 30 min, quenching in liquid nitrogen down to ~-196 °C.

E. Full-Scale Experiment Procedures

After determining the best conditions using two different types of temporary porous coating morphology based on magnesium sulfate solution which generates the highest CR and mentioned in the paragraph above, a full-scale experimental procedure was executed. The full-scale experiments included a comparison of thermal treatments accepted in conventional industry using water quenching (WQ) versus ordinary cryogenic quenching (CQ), water quenching following cryogenic quenching (WCQ), rapid cryogenic quenching into the solution of magnesium sulfate to generate temporary layer during the quenching process (SCQ1) and rapid cryogenic quenching using the solution of magnesium sulfate temporary porous layer which created at pre-austenitizing stage (SCQ2). A detailed description of the experimental procedures is presented in Table V.

In the present work, the HF (heat transfer per unit area) was calculated as in (1) based on [47]:

$$q'' = -(V/A)\,\rho C_p\,(\partial T/\partial t) \quad (1)$$

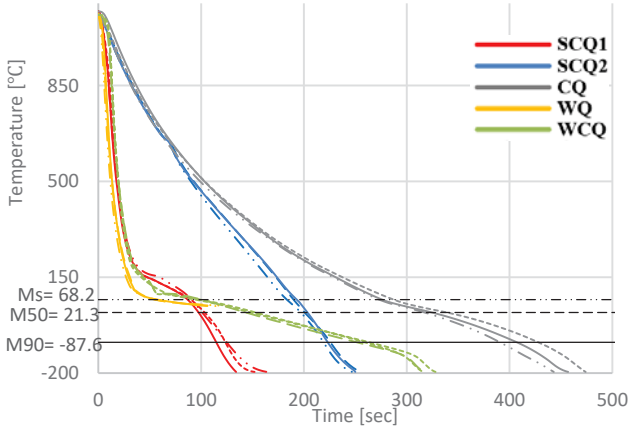

Fig. 8 Cooling curves of three repeated experiments at the same conditions for each heat treatment

III. Repeatability of the Technique

In order to approve the repeatability of the selected techniques and especially the porous coating layer creation technique, each quenching heat treatment sequence was repeated three times under the same conditions for each technique. It can be concluded that all the quenching sequences are repeatable with some slight differences due to human factor.

IV. Results and Discussion

A. Morphology Analysis of Temporary Porous Layer

In order to determine the characteristics of the porous layer form by magnesium sulfate, a CLSM examination was carried out on two different specimens which undergo a procedure of layer creation at pre-austenitizing stage (SCQ2) and during the quenching stage (SCQ1) which can be seen in Figs. 9 and 10 respectively. The following items are observed:

- In both cases the magnesium sulfate layer (Figs. 9 (a) and 10 (a)) contains non-homogeneously distributed pores with different sizes.
- In both cases the layer (Figs. 9 (b) and 10 (b)) is incomplete and areas where the surface of the specimen has been exposed can be discerned.
- A layer formed at the pre-austenitizing stage (SCQ2, Figs. 9 (a) and (b)) covers larger portion of the specimen's surface and it looks smoother and thinner than the layer formed during the quenching stage (SCQ1, Figs. 10 (a) and (b)) where the layer is characterized by distant and high "islands". This can be explained by the insufficient heat capacity of the pre-austenitizing process which allowed the magnesium sulfate solution to liquefy in the lower area of the specimen and harden there, compared to the case where the specimen had enough heat capacity to harden the larger amount of solution at the top of the specimen so that the liquid did not reach the bottom of the specimen. The type of the layer thickness and its distribution on the surface of the specimen might affect the HF at the temperatures of austenite-martensite transformation range (Fig. 12). The exact reason for this requires more in-depth research.

B. Cooling Curve for Full Quenching Processes

Typical cooling curves for the five cooling sequences are presented in Fig. 11. They show:

- The water quenching ended at approximately 25 °C, which is above the M_{50} temperature. All the other quenching processes which include the liquid nitrogen as a primary or secondary quenching media (SCQ1, SCQ2, CQ and WCQ) ended at -196 °C, which is expected to yield full austenite-martensite transformation.

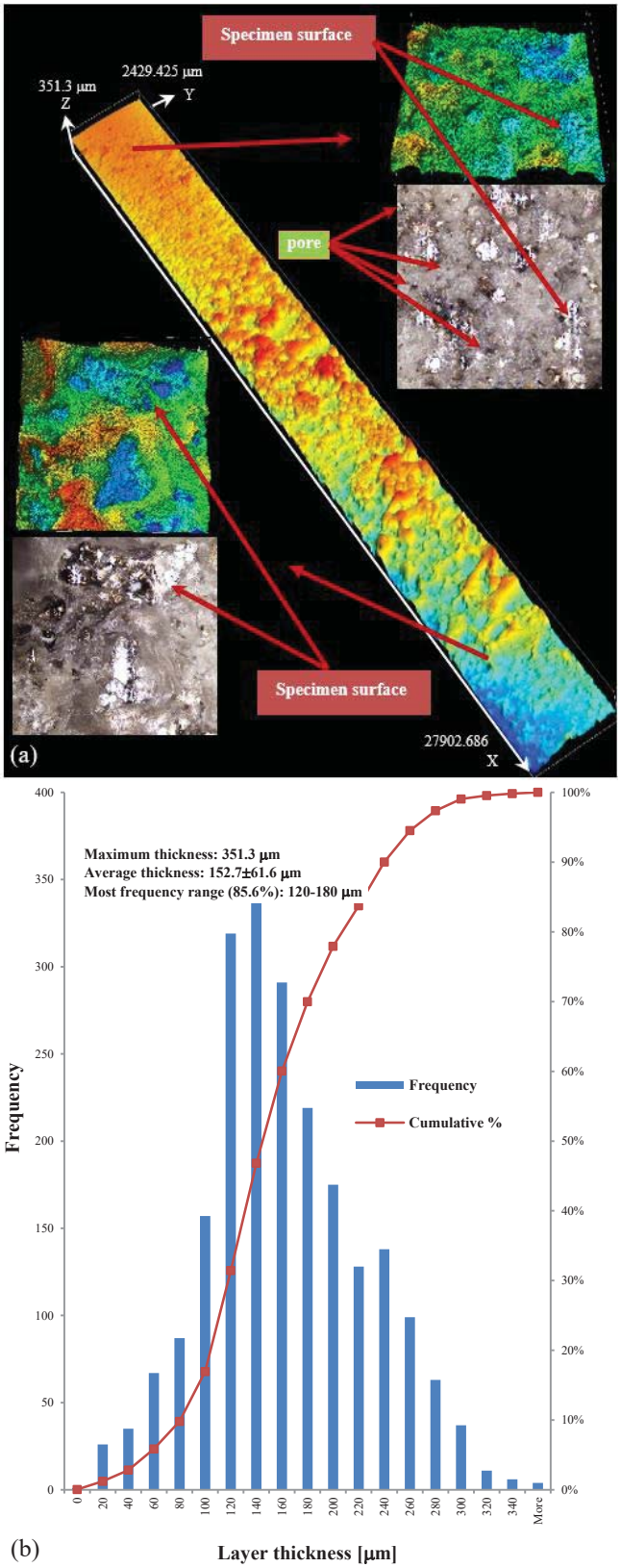

Fig. 9 Morphology of pre-austenitizing magnesium sulfate porous layer (SCQ2) obtained by CLSM in which (a) representative strip along the length of the specimen and randomly selected smaller (magnified) areas of the porous layer from top and bottom of the specimen and (b) layer thickness distribution along the selected strip

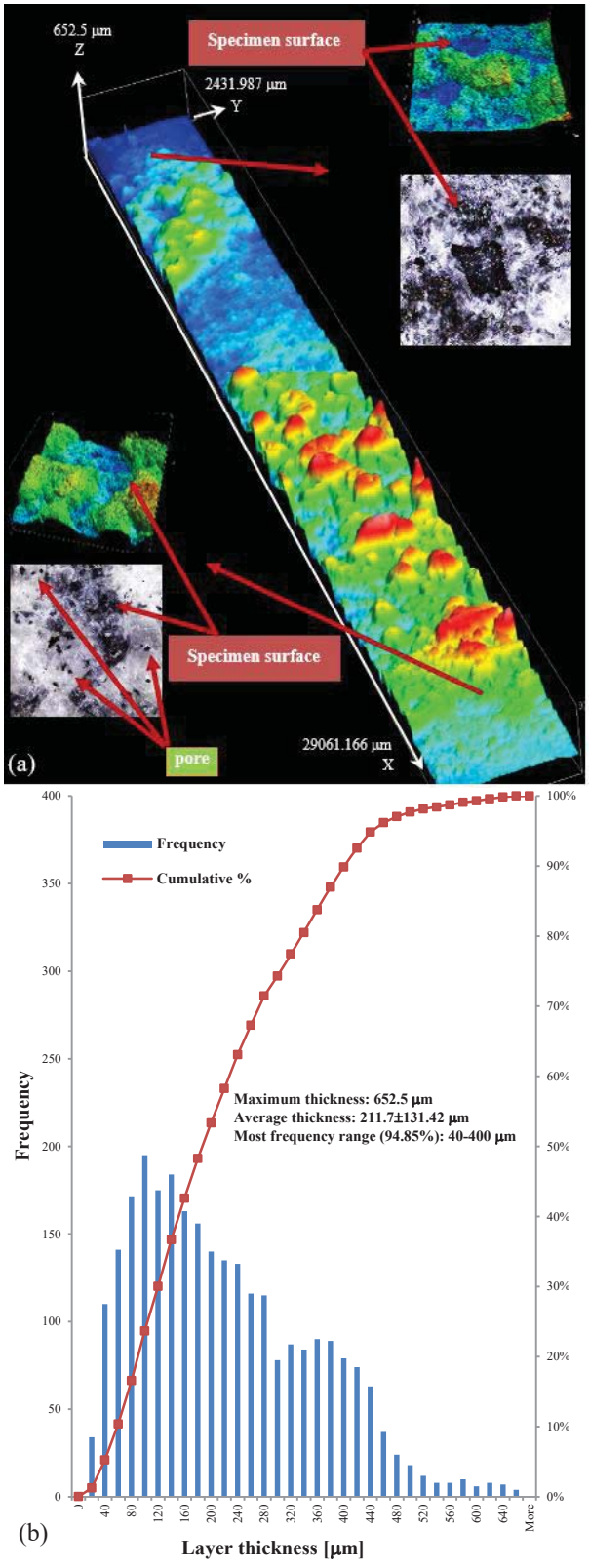

Fig. 10 Morphology of magnesium sulfate porous layer created during quenching process (SCQ1) in which (a) representative strip along the length of the specimen and randomly selected smaller (magnified) areas of the porous layer from top and bottom of the specimen and (b) layer thickness distribution along the selected strip

- All sequences which involved a coating porous layer (SCQ1 and SCQ2) produced higher HF compared to the un-coated specimens (CQ, WQ and WCQ). Moreover, the cooling curve of sequence SCQ2 is getting steeper at approximately 600 °C compared to the curve of sequence CQ in which the liquid nitrogen was used as a primary quenching media, that means that the 'Leidenfrost' temperature [48] starts already at much higher temperature (earlier stage of the quenching process). This can be explained by the capillary effect, nucleation sites and intensive bubble generation. That is, the greater and more intense contact of the liquid with the surface of the porous layer and/or the surface of the hot specimen, the greater the HF as detailed in Section I.
- Sequence SCQ1 is the most efficient followed by sequence SCQ2. But, considering the importance of the continuity of the process, sequence SCQ2 will be the most efficient.

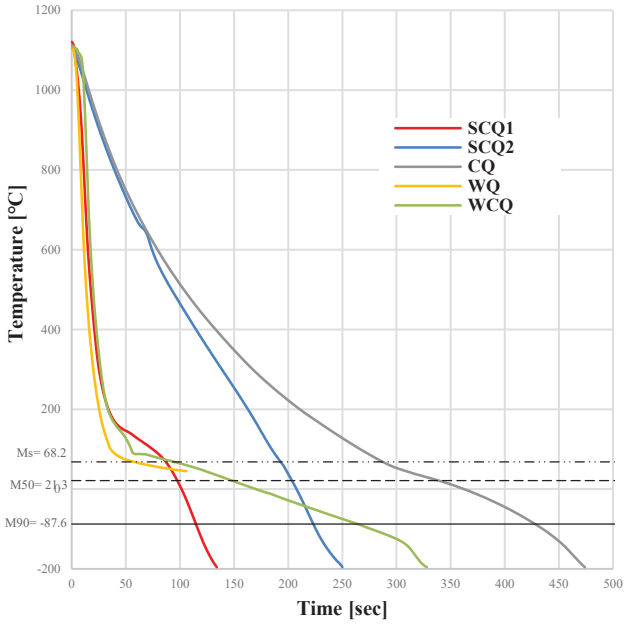

Fig. 11 Cooling curves (T-t) for quenching stage of each heat treatment process after austenitizing at 1,120 °C for 30 min

C. CR and HF at Austenite-Martensite Transformation Range

The HF as a function of temperature curves and the average HF values for the five processes are presented in Fig. 12. It confirms that all sequences which involved a coating porous layer (SCQ1 and SCQ2) produced higher HF compared to the un-coated specimens (CQ, WQ and WCQ).

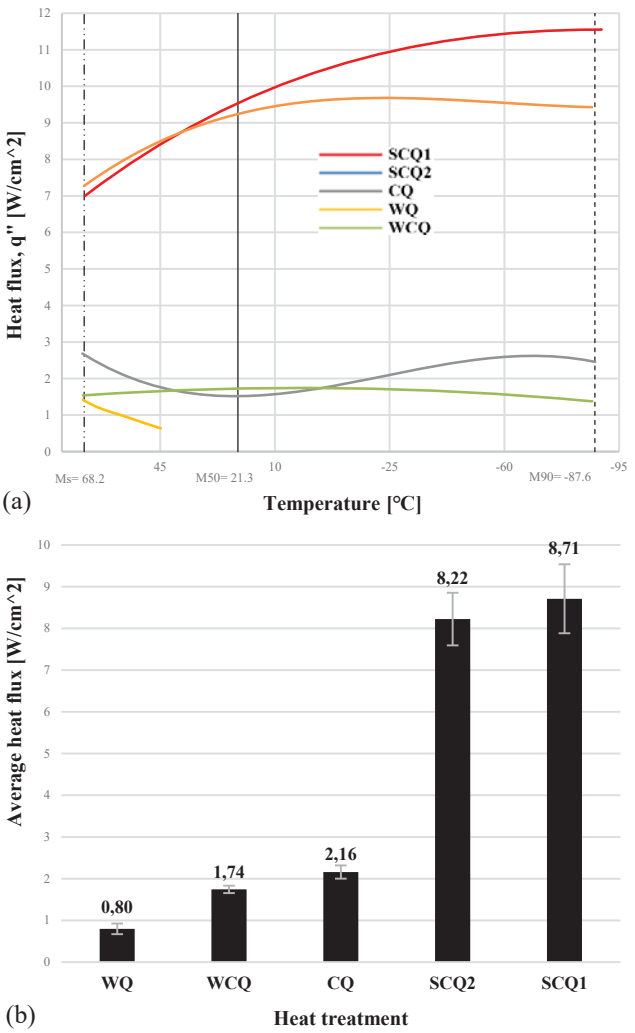

Fig. 12 HF at austenite-martensite transformation range of different quenching process after austenitizing at 1,120 °C for 30 min (a) HF curves (b) average HF values

D. Hardness

In order to determine the effect of the CR and HF gained by the temporary porous layer caused by magnesium sulfate on the hardness of the AISI D2 tool steel, the specimens were characterized as described in Section II *B*. Figs. 13 and 14 show the surface and core hardness profiles of the five types of quenching procedures. It is observed that the hardness of specimens which underwent quenching sequences with presence of temporary porous layer (SCQ1 and SCQ2) provided the highest hardness values, with the SCQ2 heat treatment sequence showed the highest surface hardness which is 967 HV10 (< 68 HRC) and sequence SCQ1 showed the highest core hardness of 885 HV10 (~66 HRC). But considering the standard deviation, it can be seen that the highest values (surface hardness and core hardness) were obtained for sequence SCQ2. This procedure also resulted with more homogeneous hardness distribution on the surface. The WQ sequence exhibits best homogeneity in the core hardness.

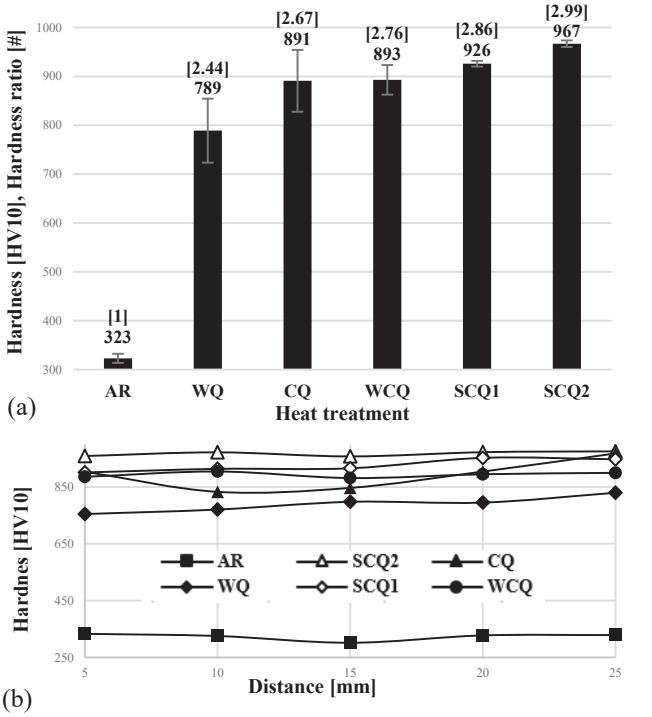

Fig. 13 Vickers hardness after austenitizing at 1,120 °C for 30 min and quenching using the different heat treatment procedures. (a) The average surface hardness and the hardness ratio (values in square brackets) between the treated and AS specimens after different heat treatments and (b) Average hardness distribution on the surface cross section of the specimens after different heat treatments. The total error did not exceed 3%

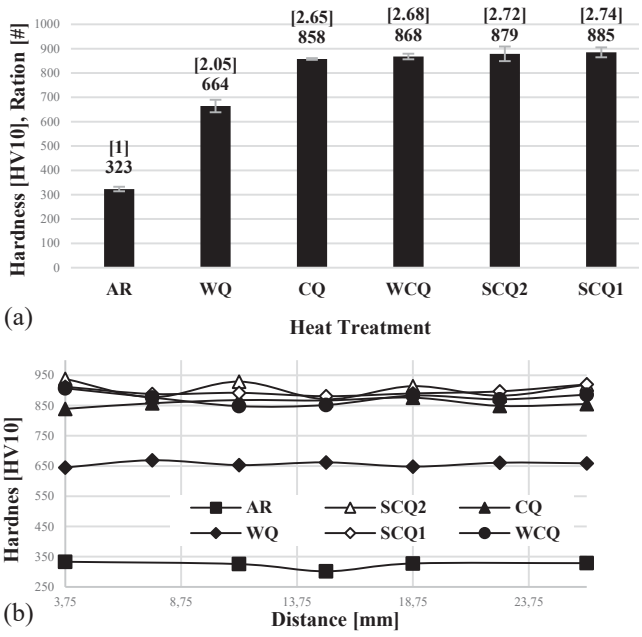

Fig. 14 Vickers hardness after austenitizing at 1,120 °C for 30 min and quenching using different heat treatments: (a) The average core hardness and the hardness ratio (values in square brackets) between the treated and AR specimens after different heat treatments; (b) The average hardness on core cross section of the specimens after different heat treatments. The total error did not exceed 3.5%

Fig. 15 illustrates the difference between the surface and the core hardness for the five quenching sequences. Except for the AR sequence, the surface hardness of the specimens is higher than its core hardness. The highest hardness ratio is obtained for specimens that have undergone water treatment (WQ).

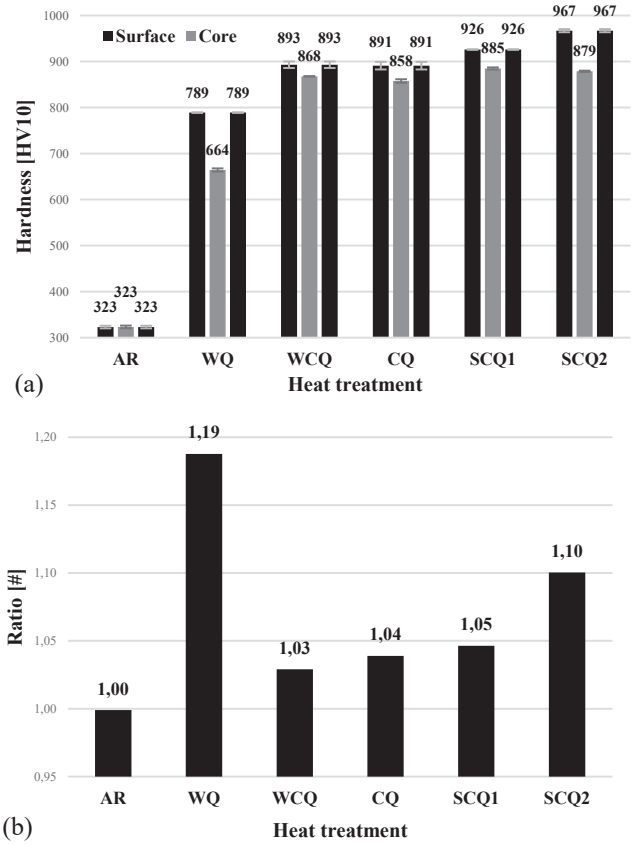

Fig. 15 Comparison of surface and core hardness after austenitizing at 1,120 °C for 30 min and quenching using different heat treatments: (a) The average surface and core hardness of each type of heat treatment; (b) The ratio of average surface hardness and the average core hardness for each type of heat treatment

V. Conclusions

The hardness of a series of AISI D2 tool steel specimens after conventional, cryogenic and rapid cryogenic heat treatments using temporary porous coating layer based on magnesium sulfate has been examined in order to evaluate the influence of those heat treatment procedures on the hardness of the steel. The obtained results and their pertinent discussion assist to infer the following:

A. All specimens that involved cryogenic heat treatment (CQ, WCQ, SCQ1 and SCQ2) showed higher hardness values compared to specimens that underwent conventional heat treatment (WQ). This is due to the fact that the temperature was dropped below the M_f temperature (-87.6 °C) fast enough.

B. Specimens that have undergone cryogenic heat treatment (CQ, WCQ, SCQ1 and SCQ2) provided a higher surface and core hardness compared with specimens which undergone a conventional heat treatment (WQ). This is probably due to a higher percentage of austenite decomposition and its transformation to martensitic structure.

C. Specimens that have undergone heat treatment with a porous coating layers based on magnesium sulfate (SCQ1 and SCQ2) have exhibited higher surface hardness compared to bare specimens that have undergone similar treatments. Although the CRs of the SCQ1 sequence were higher at high and cryogenic temperatures ranges, still, the SCQ2 quenching process showed higher hardness results. It can be deduced that continuous quenching process is preferable to quenching processes that include intermediate stops.

D. The processes which include a cryogenic treatment phase (CQ, WCQ, SCQ1 and SCQ2) provide smaller hardness differences between the specimen's surface and its core compared to conventional treatment (WQ) where the highest ratio is obtained.

E. Specimens that included a temporary coating layer showed higher and more homogeneous CRs and HFs compared to the other processes.

F. The technique of temporary porous layer creation based on magnesium sulfate is repeatable and can be used as a primary (SCQ2) or secondary (SCQ1) method in quenching processes for cryogenic heat treatments.

G. The CRs using temporary porous layer (SCQ1 and SCQ2) are low cost and controllable, by changing the condition of its creation (solution concentration, initial temperature of the solution, initial and final temperature of the dipped specimen inside the solution and the dipping time of the specimen inside the solution) a different porous layer morphology (layer thickness, size and distribution of the pores) is obtained which effects the boiling regimes and the CRs.

Acknowledgment

A. Rabin would like to thank Dr. Alex Shapiro from the Department of Physics and the Department of Mechanical Engineering at the Shamoon College of Engineering, Beer Sheva Campus for the tremendous help and professional guidance in analyzing part of the results of the research. We also would like to thank Mr. Nikolay Razoronov from the Department of Mechanical Engineering at Shamoon College of Engineering, Beer Sheva Campus for the technical help in conducting the experiments.

References

[1] "Industeel D2," ArcelorMittal, 11 February 2022. (Online). Available: https://industeel.arcelormittal.com/fichier/ds-tool-d2/.

[2] N. Pillai, R. Karthikeyan and P. J. Davim, "A Review on Effect of Cryogenic Treatment of AISI 'D' Series Cold Working Tool Steels," Rev. Adv. Mater. Sci, vol. 51, pp. 149-159, 2017.

[3] M. Villa and M. A. J. Somers, "Cryogenic treatment of an AISI D2 steel: The role of isothermal martensite formation and "martensite conditioning"," vol. 110, pp. 1-6, September 2020.

[4] S. Harpreet, S. Rupinder, S. Jagdev and S. G. Simranpreet, "Cryoprocessing of cutting tool materials—a review," The International

Journal of Advanced Manufacturing Technology, vol. 48, pp. 175-192, 2010.

[5] A. Oppenkowskia, S. Weber and W. Theisen, "Evaluation of factors influencing deep cryogenic treatment that affect the properties of tool steels," Journal of Materials Processing Technology, vol. 210, pp. 1949-1955, 2010.

[6] V. G. Gavriljuk, W. Theisen, V. V. Sirosh, E. V. Polshin, A. Kortmann, G. S. Mogilny, Y. N. Petrov and Y. V. Tarusin, "Low-temperature martensitic transformation in tool steels in relation to their deep cryogenic treatment," Acta Materialia, vol. 61, pp. 1705-1715, 2013.

[7] C. A. B. H. G. Paula Fernanda da Silva Farina, "Microstructural Characterization of an AISI D2 Tool Steel Submitted to Cryogenic Treatment," Journal of ASTM International, vol. 8, no. 5, pp. 1-8, May 2011.

[8] D. Das and K. K. Ray, "On the mechanism of wear resistance enhancement of tool steels by deep cryogenic treatment," Philosophical Magazine Letters, vol. 92, no. 6, pp. 295-303, June 2012.

[9] H. Ghasemi-Nanesa and M. Jahazi, "Simultaneous enhancement of strength and ductility in cryogenically treated AISI D2 tools teel," Materials Science & Engineering A, vol. 598, pp. 413-419, 2014.

[10] D. Das, A. K. Dutta and K. K. Ray, "Sub-zero treatments of AISI D2 steel: Part I. Microstructure and hardness," Materials Science and Engineering A, vol. 527, pp. 2182-2193, 2010.

[11] D. Das, A. K. Dutta and K. K. Ray, "Sub-zero treatments of AISI D2 steel: Part II. Wear behavior," Materials Science and Engineering A, vol. 527, pp. 2194-2206, 2010.

[12] P. F. George E. Totten, Ed., Steel Heat Treatment Handbook., 2nd Edition ed., Portland, Oregon: Taylor&Francis group, 2006, pp. 95-97, 179-181.

[13] I. N. Kobasko, G. E. Totten and L. Canale, "Mechanism of Surface Compressive Stress Formation by Intensive Quenching," in MECOM 2005 - VIII Congreso Argentino de Mecánica Computacional, Buenos Aires, Argentina, 2005.

[14] N. I. Kobasko, J. A. Powell, M. A. Aronov, L. C. Canale and G. E. Totten, "Intensive Quenching Process Classification and Applications," Jinshu Rechuli/Heat Treatment of Metals, vol. 31, no. 3, pp. 51-58, January 2004.

[15] M. A. S. Matteo Villa, "Cryogenic treatment of steel: from concept to metallurgical understanding," in 24th IFHTSE Congress 2017 European Conference on Heat Treatment and Surface Engineering A3TS CONGRESS, 2017.

[16] I. Starodubsteva and A. N. Pavlenko, "The Evolution of Temperature Disturbances During Boiling of Cryogenic Liquids on Heat-Releasing surfaces," Evaporation, Condensation and Heat transfer, pp. 95-122, 12 September 2011.

[17] Y. Liu, T. Olewski, L. Vechot, X. Gao and S. Mannan, "Modelling of a cryogenic liquid pool boiling using CFD code," in 14th Annual Symposium, Texas, 2011.

[18] H. Hu, C. Xu, Y. Zhao, Z. J. Ziegler and J. N. Chung, "Boiling and quenching heat transfer advancement by nanoscale surface modification," Scientific Reports, vol. 7, no. 1, pp. 1-16, 21 July 2017.

[19] D. D. Hall and I. Mudawar, "Critical heat flux (CHF) for water flow in tubes - I. Compilation and assesment of world CHF data," International Journal of Heat and Mass Transfer, vol. 47, pp. 2573-2604, 2000.

[20] G. Liang and I. Mudawar, "Pool boiling critical heat flux (CHF) – Part 1: Review of mechanisms, models, and correlations," International Journal of Heat and Mass Transfer, vol. 117, pp. 1352-1367, 2018.

[21] A. Bergles, "High-Flux Processes Through Enhanced Heat Transfer," in Keynote 5th Int. Conf. BoilingHeat Transfer, Montego Bay, Jamaica, 2003.

[22] A. Monnot, P. Boldo, N. Gondrexon and A. Bontemps, "Enhancement of Cooling Rate by Means of High Frequency Ultrasound," Heat Transfer Engineering, vol. 1, no. 28, pp. 3-8, 2007.

[23] M. Legay, N. Gondrexon, S. Le Person, P. Boldo and A. Bontemps, "Enhancement of Heat Transfer by Ultrasound: Review and Recent Advances," International Journal of Chemical Engineering, vol. 2011, pp. 1-17, 20 07 2011.

[24] M. Jadhav, R. Awari, D. Bibe, A. Bramhane and M. Mokashi, "Review on Enhancement of Heat Transfer by Active Method," International Journal of Current Engineering and Technology, no. Special Issue-6, pp. 221-225, 2016.

[25] L. Leal, M. Muscevic, P. Lavieille, M. Amokrane, F. Pigache, F. Topin, B. Nogarede and L. Tadrist, "An overview of heat transfer enhancement methods and new perspectives: Focus on active methods using electroactive materials," International Journal of Heat and Mass Transfer, vol. 61, pp. 505-524, June 2013.

[26] I. Mudawar and G. Liang, "Review of pool boiling enhancement with additives and nanofluids," vol. 124, pp. 423-453, 09 2018.

[27] T. Sonawane, P. Patil, A. Chavhan and B. Dusane, "A Review on Heat Transfer Enhancement by Passive Methods," International Research Journal of Engineering and Technology (IRJET), vol. 3, no. 9, pp. 1567-1574, 09 2016.

[28] R. Pastuszko and T. M. Wójcik, "Experimental investigations and a simplified model for pool boiling on micro-fins with sintered perforated foil," Experimental Thermal and Fluid Science, vol. 63, pp. 34-44, May 2015.

[29] D. Saeidi, A. A. Alemrajabi and N. Saeidi, "Experimental study of pool boiling characteristic of an aluminized copper surface," International Journal of Heat and Mass Transfer, vol. 85, pp. 239-246, June 2015.

[30] S. K. Gupta and R. D. Misra, "Experimental study of pool boiling heat transfer on copper surfaces with Cu-Al2O3 nanocomposite coatings," International Communications in Heat and Mass Transfer, vol. 97, pp. 47-55, October 2018.

[31] X. Kong, Y. Zhang and J. Wei, "Experimental study of pool boiling heat transfer on novel bistructured surfaces based on micro-pin-finned structure," Experimental Thermal and Fluid Science, vol. 91, pp. 9-19, 2018.

[32] S. H. Kim, G. C. Lee, J. Y. Kang, K. Moriyama, M. H. Kim and H. S. Park, "Boiling heat transfer and critical heat flux evaluation of the pool boiling on micro structured surface," International Journal of Heat and Mass Transfer, vol. 91, pp. 1140-1147, 2015.

[33] S. G. Liter and Kaviany, "Pool-boiling CHF enhancement by modulated porous-layer coating: theory and experiment," International Journal of Heat and Mass Transfer, vol. 44, pp. 4287-4311, 12 January 2001.

[34] Y.-Q. Wang, S.-S. Lyu, J.-L. Luo, Z.-Y. Luo, Y.-X. Fu, Y. Heng, J.-H. Zhang and D.-C. Mo, "Copper vertical micro dendrite fin arrays and their superior boiling heat transfer capability," Applied Surface Science, vol. 422, pp. 388-393, 30 May 2017.

[35] S. Sarangi, J. A. Weibel and S. V. Garimella, "Effect of particle size on surface-coating enhancement of pool boiling heat transfer," International Journal of Heat and Mass Transfer, vol. 81, pp. 103-113, 2015.

[36] S. Jun, J. C. Godinez, S. M. You and H. Y. Kim, "Pool boiling heat transfer of a copper microporous coating in borated water," Nuclear Engineering and Technology, vol. 52, pp. 1939-1944, 2020.

[37] Y.-Q. Wang, J.-L. Luo, Y. Heng, D.-C. Mo and S.-S. Lyu, "Wettability modification to further enhance the pool boiling performance of the micro nano bi-porous copper surface structure," International Journal of Heat and Mass Transfer, vol. 119, pp. 333-342, 2018.

[38] D. He, P. Zhang, F. Lv, S. Wang and D. Shu, "Cryogenic quenching enhancement of a nanoporous surface," International Journal of Heat and Mass Transfer, vol. 134, pp. 1061-1072, 05 February 2019.

[39] H. Hu, C. Xu, Y. Zhao, R. Shaeffer, K. J. Ziegler and J. Chung, "Modification and enhancement of cryogenic quenching heat transfer by a nanoporous surface," International Journal of Heat and Mass Transfer, vol. 80, pp. 636-643, 15 October 2014.

[40] J. Chung, S. Darr, J. Dong, H. Wang and J. Hartwig, "Heat transfer enhancement in cryogenic quenching process," International Journal of Thermal Sciences, vol. 147, p. 106117, January 2020.

[41] A. Rabin, G. Mazor, A. Shapiro, R. Z. Shneck and I. Ladizhenski, "Mechanical and Electrical Properties of AISI D2 steel and Pure Copper After Cryogenic Treatment," in the 35th Israel Conference of Mechanical Engineering, Beer-Sheva, 2018.

[42] G. Mazor, E. Korin, D. Nemirovsky and I. Ladizhensky, "Frost formation as a temporary enhancer for quench pool boiling," Applied Thermal Engineering, vol. 52, no. 2, pp. 345-352, 2013.

[43] I. Ladizhensky, E. Korin, G. Mazor, D. Nemirovsky and E. Goldkin, "Quench pool boiling with temporary crystalline enhancers, (2014), Volume:37, Issue:2, pp.349-356," Chemical Engineering & Technology, vol. 37, no. 2, pp. 349-356, February 2014.

[44] G. Mazor, I. Ladizhensky, A. Shapiro and D. Nemirovsky, "Modification of pool boiling regimes by sand deposition," Heat Transfer, vol. 49, pp. 1000-1015, 2020.

[45] A. Rabin, G. Mazor, R. Z. Shnek, I. Ladizhanski and A. Shapiro, "Effect of Cryogenic Cooling Rate on the Tool Steels Properties," in IMEC-18. Israel Materials Ingineeiring Conference, Dead Sea, Israel, 2018.

[46] D. Bomac, A. Podeer, M. Fazarinc and G. Kugler, "Study of Carbide Evolution During Thermo-Mechanical Processing of AISI D2 Tool Steel," Materials Engineering and Performance, vol. 22, no. 3, pp. 742-747, March 2013.

[47] A. E. Bergles and W. G. J. Thompson, "The Relationship of Quench Data to Steady-State Pool Boiling Data," International Journal of Heat Mass Transfer., vol. 13, pp. 55-68, 17 March 1969.
[48] R. Jeschar, E. Specht and C. Kohler, "Heat Transfer During Cooling of Heated Metallic Objects with Evaporating Liquids," in Theory and Technology of Quenching, B. Liscic, H. M. Tensi and W. Luty, Eds., New York, Springer Science+ Business Media, LLC, 1992, pp. 73-88
[49] N. I. Kobasko, Intensive Steel Quenching Methods, B. Liscic, H. M. Tensi and W. Luty, Eds., New York: Springer Science+ Business Media, LLC, 1992, p. 367.